

Interstrand crosslink-induced homologous recombination carries an increased risk of deletions and insertions

Vidya S. Jonnalagadda, Tetsuya Matsuguchi, Bevin P. Engelward*

Biological Engineering Division, Massachusetts Institute of Technology, 77 Massachusetts Ave., 56-631, Cambridge, MA 02139, USA

Received 4 February 2005; accepted 4 February 2005

Abstract

Homology directed repair (HDR) defends cells against the toxic effects of two-ended double strand breaks (DSBs) and one-ended DSBs that arise when replication progression is inhibited, for example by encounter with DNA lesions such as interstrand crosslinks (ICLs). HDR can occur via various mechanisms, some of which are associated with an increased risk of concurrent sequence rearrangements that can lead to deletions, insertions, translocations and loss of heterozygosity. Here, we compared the risk of HDR-associated sequence rearrangements that occur spontaneously versus in response to exposure to an agent that induces ICLs. We describe the creation of two fluorescence-based direct repeat recombination substrates that have been targeted to the ROSA26 locus of embryonic stem cells, and that detect the major pathways of homologous recombination events, e.g., gene conversions with or without crossing over, repair of broken replication forks, and single strand annealing (SSA). SSA can be distinguished from other pathways by application of a matched pair of site-specifically integrated substrates, one of which allows detection of SSA, and one that does not. We show that SSA is responsible for a significant proportion of spontaneous homologous recombination events at these substrates, suggesting that two-ended DSBs are a common spontaneous recombinogenic lesion. Interestingly, exposure to mitomycin C (an agent that induces ICLs) increases the proportion of HDR events associated with deletions and insertions. Given that many chemotherapeutics induce ICLs, these results have important implications in terms of the risk of chemotherapy-induced deleterious sequence rearrangements that could potentially contribute to secondary tumors.

© 2005 Elsevier B.V. All rights reserved.

Keywords: Mitotic homologous recombination; Interstrand crosslinks; Single strand annealing; Direct repeat; Mouse ES cells

1. Introduction

Endogenous and exogenous DNA damaging agents create thousands of DNA lesions per cell each day. Lesions that affect just one strand of the DNA duplex are generally repaired by excision of the damaged nucleotide(s) and replacement using the intact complementary strand as a template [1]. However, if both strands are damaged (e.g., by a double strand break [DSB]), another source of sequence information is required for accurate repair. Homology directed repair (HDR) allows cells to use the undamaged sister chromatid or the homologous chromosome as a template for repair. In addition, HDR can reconstitute broken replication forks by

accurately reinserting the broken DNA end into the sister chromatid [2–6].

HDR often occurs via a relatively conservative pathway in which there is a non-reciprocal transfer of sequence information at the site of the original damage, without exchange of flanking sequences (e.g., gene conversion without crossing over). However, some HDR events are associated with crossovers, and crossovers between misaligned sister chromatids inevitably lead to gains and losses of sequence information. In cases where HDR occurs between homologous chromosomes, even if there is accurate alignment, crossovers can lead to loss of heterozygosity along vast stretches of the chromosome (from the exchange point to the telomere).

It is thought that most homologous recombination events are initiated by two-ended DSBs and one-ended DSBs. Two-ended DSBs can be created at any time during the cell cycle by agents that destroy the integrity of the sugar-phosphate

* Corresponding author. Tel.: +1 617 258 0260; fax: +1 617 258 0499.
E-mail address: bevin@mit.edu (B.P. Engelward).

backbone or by agents that induce damage that is subsequently enzymatically cleaved (e.g., base excision repair of closely opposed lesions can lead to DSBs [7]). On the other hand, one-ended DSBs are completely replication dependent, arising when replication forks encounter lesions that inhibit progression. While some lesions can directly disintegrate the fork (e.g., encounter with single strand nicks or gaps), other lesions can indirectly cause replication forks to breakdown by stalling progression, which can lead to formation of a Holliday junction that is prone to enzymatic cleavage (for excellent recent reviews on this subject, the reader is referred to [4,5,8]).

For all DSBs, one of the earliest steps of HDR is resection of the DNA end(s) to create a 3' overhang that becomes bound by Rad51 and associated factors, forming a nucleoprotein filament capable of homology searching [2–6]. This filament can invade homologous sequences and undergo repair synthesis using a homologous duplex DNA as a template. In the prototypic break repair model, as first proposed by Szostak et al., both ends of a two-ended DSB invade the homologous sequence, forming two Holliday junctions that, when cleaved, lead to exchange of flanking sequences 50% of the time [9]. Alternatively, Holliday junction cleavage can be avoided via synthesis dependent strand annealing (SDSA), wherein translocation of a Holliday junction releases a DNA end, which can then anneal to the other end of the break [10,11]. In addition to the prototypic break-repair and SDSA models, DSBs at repeated sequences can also be repaired by single strand annealing (SSA), a subpathway of homologous recombination where the resected single stranded regions simply anneal to one another, without invading a homologous duplex DNA [12,13]. This pathway inevitably leads to loss of one copy of the repeated sequences. We define a homologous recombination event in which there is an associated gain or loss of sequences to be non-conservative, since the original arrangement of the DNA has been lost.

It is well established that conditions that lead to increased levels of HDR are associated with an increased risk of cancer [14,15]. Indeed, many known carcinogens are potent recombinogens, including oxidizing agents, alkylating agents, UV light, and ionizing radiation [16–18]. Although the mechanisms of recombination initiated by homing endonucleases that introduce two-ended DSBs are well studied (e.g., [19–23]), to our knowledge, there are only two studies reporting the mechanisms of recombination induced by other types of DNA damaging agents in mammalian cells [24,25]. We are particularly interested in the possibility that carcinogens not only can induce HDR, but that exposure may skew the distribution of events in favor of non-conservative HDR events that are associated with deletions and insertions. Among known carcinogens, agents that induce interstrand crosslinks (ICLs) are highly recombinogenic in mammalian cells [26–29]. ICLs interfere with normal DNA replication by preventing strand separation, and it is thought that ICLs induce HDR primarily by inducing replication fork breakdown, resulting in the formation of one-ended DSBs [30]. This model is supported by

two studies showing that the majority of ICL-induced DSBs arise in a replication-dependent fashion [31–33]. Thus, by investigating the types of sequence rearrangements induced by ICLs, we can learn about the relative risk of deleterious sequence rearrangements induced by an agent that is thought to primarily cause replication-dependent one-ended DSBs.

A common approach for studying HDR is to use direct repeat substrates in which recombination restores expression of a selectable marker. Many such substrates detect SSA, but SSA events are not generally discernable from other classes of recombination events, such as unequal sister chromatid exchanges. Here we describe the creation and application of two site-specifically integrated direct repeat substrates to study both spontaneous and damage-induced recombination in non-transformed mammalian cells. Both substrates detect gene conversions (with and without crossing over) and HDR events associated with repair of broken fork. However, only one of the substrates detects SSA, thus providing a strategy to estimate the contribution of SSA. We found that ~50–65% of spontaneous recombination events are due to conservative HDR (e.g., gene conversions without crossing over), which is consistent with previously published reports indicating that most spontaneous HDR events are conservative gene conversions [28,29,34–36]. In addition, we provide some of the first direct evidence that SSA is a frequent spontaneous homologous recombination event at direct repeats in mammalian cells, which suggests that endogenously induced two-ended DSBs are the underlying cause of a significant portion of spontaneous homologous recombination events. When comparing spontaneous recombination events to those induced by exposure to an agent that forms ICLs, we find that most ICL-induced recombination events are non-conservative, thus putting cells at an increased risk of deleterious rearrangements. These results have important implications to cancer patients who are frequently treated with chemicals that induce ICLs.

2. Materials and methods

2.1. Enzymes, oligonucleotides, plasmids

Restriction enzymes were from New England Biolabs (Beverly, MA). Hotstart polymerase (Eppendorf International) was used for diagnostic PCR, and Advantage2 polymerase (BD Biosciences, CA) was used in construction. Oligonucleotides were from Amifit Inc. (Allston, MA). Tissue culture reagents were from Gibco/BRL. Plasmid pCX-EGFP was a gift from Okabe et al. [37], and plasmids pBigT and pROSA26PA were gifts from Soriano [38] and Srinivas et al. [39]. Oligonucleotide and vector sequences are available upon request.

2.2. Construction of recombination substrates

The *PstI*–*Bam*HI fragment in pCX-EGFP was replaced with a synthetic adaptor carrying *Nsi*I, *Not*I and *Xho*I sites,

and the coding sequences for enhanced green fluorescent protein (EGFP) removed by digestion with *EcoRI* to obtain pCX-NNX. Full length and truncated coding sequences ($\Delta 5egfp$, lacking sequences at the 5' end, and $\Delta 3egfp$, lacking sequences from the 3' end) for EGFP were amplified by PCR from pCX-EGFP using primers carrying *ApoI* sites. In $\Delta 5egfp$, this resulted in a removal of 27 bp (of which 15 were in the coding region), which were replaced with 31 bp of unique sequence. In $\Delta 3egfp$, this resulted in a removal of 93 bp (of which 81 were in coding sequence), which were replaced with 62 bp of unique sequence. *ApoI* digested PCR products were subcloned into *EcoRI* digested pCX-NNX to obtain pCX-NNX-EGFP, pCX-NNX- $\Delta 5egfp$ and pCX-NNX- $\Delta 3egfp$. The expression cassettes (promoter, enhancer, intron, coding and polyadenylation sequences) from pCX-NNX- $\Delta 5egfp$ and pCX-NNX- $\Delta 3egfp$ were released with *SalI* and *PstI*. The cassettes were cloned into *NsiI* and *XhoI*-digested pCX-NNX- $\Delta 3egfp$ and pCX-NNX- $\Delta 5egfp$, respectively, to obtain pCX-NNX- ΔGI and pCX-NNX- ΔGF . Plasmid pBigT-TpA [39] was derived from pBigT by removal of the 1 kb *HindIII*–*NheI* fragment. Expression cassettes from plasmids pCX-NNX-EGFP, pCX-NNX- $\Delta 5egfp$, pCX-NNX- $\Delta 3egfp$, pCX-NNX- ΔGI and pCX-NNX- ΔGF were released by *SalI* and *NotI*, and cloned into pBigT-TpA digested with *SalI* and *NotI*. Each of these plasmids was digested with *AscI* and *PacI* to release the corresponding expression cassettes, which were then cloned into pROSA26PA digested with *AscI* and *PacI*. Restriction enzymes were used to linearize all five plasmids: pROSA26-EGFP (*KpnI*), pROSA26- $\Delta 5egfp$ (*KpnI*), pROSA26- $\Delta 3egfp$ (*PvuII*), pROSA26- ΔGI (*XhoI*) and pROSA26- ΔGF (*XhoI*). Linearized plasmids were electroporated into mouse embryonic stem (ES) J1 cells (gift of R. Jaenisch, MIT). Clones selected for resistance to neomycin (DMEM containing 15% fetal bovine serum, penicillin, streptomycin and glutamine, LIF, containing G418) were tested by PCR and Southern blotting for correct targeting of the expression cassettes into the ROSA26 locus.

2.3. Southern blotting and PCR analysis

For Southern blotting, genomic DNA was digested with *EcoRV* and probed using a previously described small fragment that lies outside of the targeting vector [38,39]. Correctly targeted clones were further analyzed by Southern blotting using at least two independent diagnostic digestions followed by probing with EGFP sequences. Only clones that showed both correct targeting and a single integration event were used in subsequent studies. PCR testing of targeting of insert to the ROSA26 locus was done using primers that yield a product of 1.2 kb exclusively at the targeted allele [38] (see also <http://www.fhcr.org/labs/soriano/rosa26.htm>). To analyze recombinant clones, PCR primers were designed to exclusively amplify EGFP, $\Delta 5egfp$ and $\Delta 3egfp$, as described in Section 3 (primer sequences are available upon request). Template was added to two reactions that were always

performed in parallel, one to assay for EGFP, and the other to assay for $\Delta 5egfp$ and $\Delta 3egfp$.

2.4. Flow cytometry for analysis and isolation of recombinant cells

Trypsinized cells were resuspended in OptiMEM and analyzed on a Becton Dickinson FACScan flow cytometer (excitation 488 nm, argon laser). Fluorescent cells were sorted using a MoFlo cytometer (Cytomation Inc.; excitation 488 nm, argon laser; emission 580/30). Live cells were gated using forward and side scatter. Recombinant cells were sorted into gelatin coated tissue culture plates and single clones expanded for PCR and Southern blotting.

2.5. Rate of spontaneous recombination

Independent cultures were initiated with $\sim 2 \times 10^4$ cells (or fewer) and the frequency of fluorescent recombinant cells was determined by flow cytometry after 48–72 h. Samples with frequencies of recombinant cells consistent with the presence of a fluorescent cell at the time of plating were excluded from subsequent analysis, and the rate of recombination and standard deviations were calculated as previously described using the MSS Method of Maximum Likelihood [40].

2.6. Toxicity and frequency of recombinant cells in ICL-exposed cultures

Cells (~ 0.5 – 2×10^6) were plated in gelatinized six-well plates. After 24 h, the cells were exposed to Mitomycin C (MMC) in DMEM for 1 h. Samples were analyzed by flow cytometry after 48–72 h (~ 3 – 4 population doublings in control cells). Population growth relative to untreated control cells was estimated by Coulter Counting.

2.7. Sister chromatid exchange analysis

Sister chromatid exchanges were counted in metaphase spreads as previously described [41]. Briefly, cells were grown for 24 h in medium containing BrdU, and colcemid was added for the last 3 h. Trypsinized cells were suspended in hypotonic solution, fixed in Carnoy's solution, and dropped onto slides. Metaphase spreads were stained with Hoechst 33258 and Giemsa. Over 20 metaphase spreads were analyzed for each sample.

3. Results

3.1. Recombination substrate construction and targeted integration

To create homologous recombination substrates, we modified an expression cassette for EGFP [37] (Fig. 1(A))

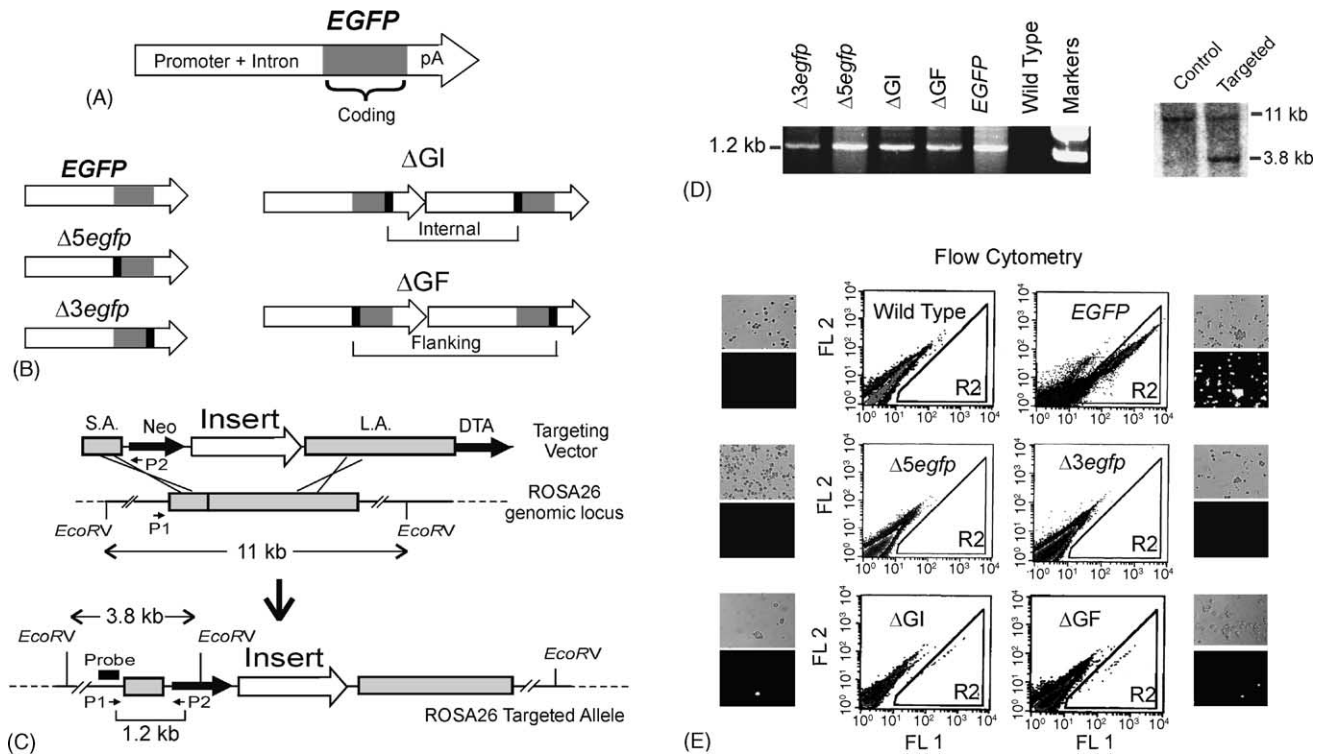


Fig. 1. Construction of direct repeat recombination substrates. (A) Features of the *EGFP* expression cassette. Expression is driven by the chicken β -actin promoter with the cytomegalovirus enhancer; pA, polyadenylation sequence. Drawn to scale where the total length = ~ 3 kb. (B) Expression cassettes targeted to the ROSA26 locus. Arrows indicate the cassette, gray regions indicate coding sequences and black boxes indicate deletions (deletions not to scale). (C) Diagram showing the targeting approach for the ROSA26 locus, as has been previously described [39]. S.A. and L.A., short arm and long arm of ROSA26 genomic sequences; Neo, neomycin; DTA, diphtheria toxin A; insert, each of the five different inserts is shown in 'B'; P1 and P2, primers that yield a 1.2 kb product exclusively for the targeted allele. The probe used for Southern blotting is indicated, and falls outside of the targeting vector, yielding a 3.8 kb *EcoRV* fragment unique to the correctly targeted allele. (D) Examples of PCR and Southern blotting results for correctly targeted clones. *Left*: PCR identification of targeted clones showing a 1.2 kb product diagnostic of the targeted allele. *Right*: Representative Southern blotting showing *EcoRV* digested genomic DNA from a correctly targeted clone. (E) Images show phase contrast and fluorescence microscopy. Flow cytometry plots indicate the relative fluorescence intensity for 515–545 nm (FL1) vs. 562–588 (FL2). The R2 region was delineated to capture most fluorescent cells while excluding non-fluorescent cells.

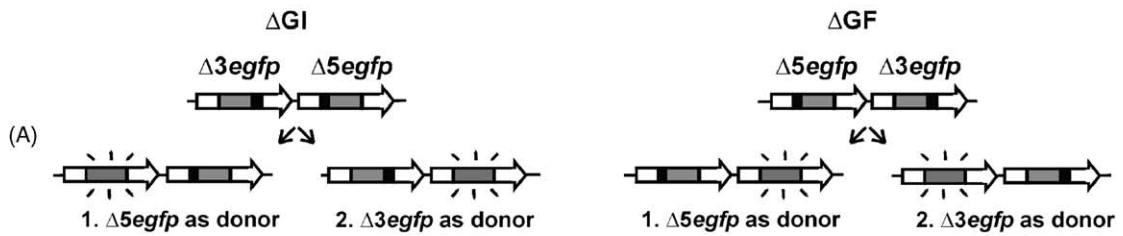
to create two different truncated *egfp* expression cassettes. DNA sequences for amino acid residues shown to be essential for fluorescence [42] were deleted, such that the coding sequence lacks 15 bp at the 5' end in $\Delta 5egfp$ (including the start codon), and 81 bp at the 3' end in $\Delta 3egfp$ (Fig. 1(B)). The truncated coding sequences are flanked by >500 bp of identical sequences that include an intron, polyadenylation signal sequences, and a promoter known to yield high levels of expression in mice. These deleted cassettes were then ligated in tandem in two arrangements. In ΔGI (deleted green internal), $\Delta 5egfp$ is downstream of $\Delta 3egfp$ such that the deletions are positioned internally, relative to the coding sequences (Fig. 1(B)). In ΔGF (deleted green flanking), $\Delta 5egfp$ is placed upstream of $\Delta 3egfp$, such that the deletions are flanking the coding sequences (Fig. 1(B)). The rationale behind this approach is that SSA can restore a full length *EGFP* in ΔGI , but not in ΔGF (Fig. 2(D)). Therefore, by comparing the rates of recombination in this pair of substrates, we can estimate the rate of SSA.

It is well established that the spontaneous rate of recombination depends upon the locus of integration [36]. Therefore, in order to reveal the extent of SSA, ΔGI and ΔGF needed

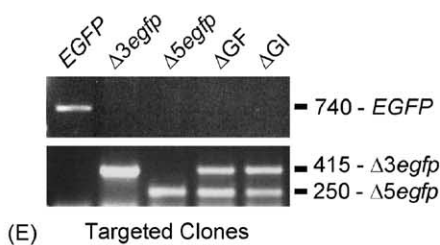
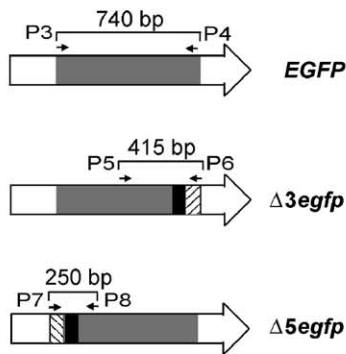
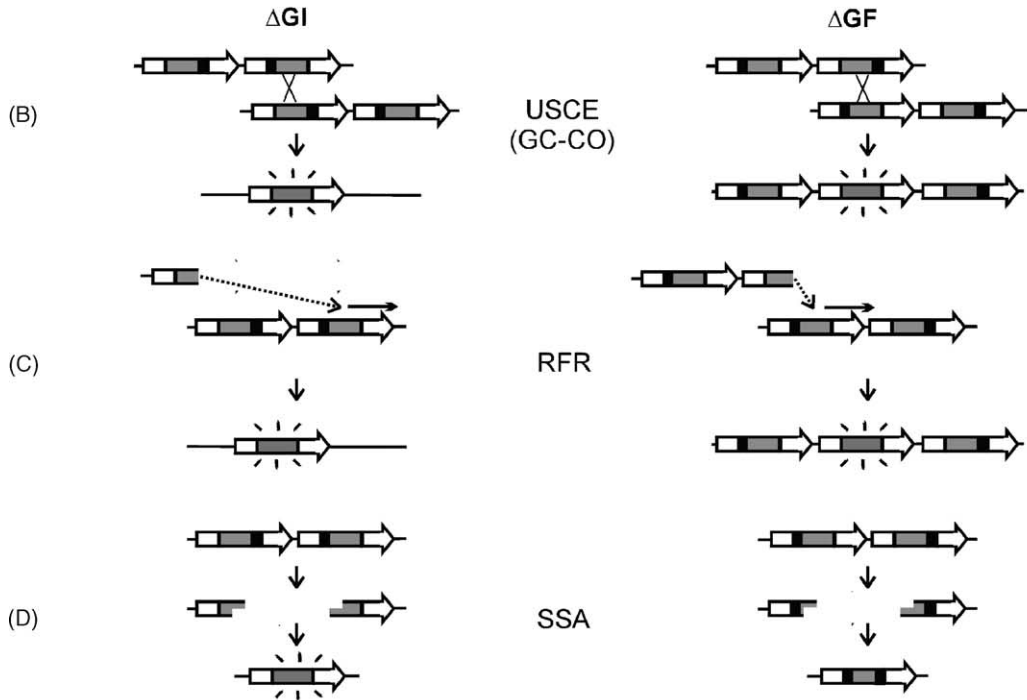
to be integrated into an identical locus. Using a previously described targeting system [38,39], each of the three control cassettes and the two recombination substrates were individually ligated into a ROSA26 targeting vector (Fig. 1(C)) and electroporated into mouse embryonic stem (ES) cells. Correctly targeted clones were identified by a diagnostic PCR reaction that yields a 1.2 kb fragment uniquely present in the targeted alleles (Fig. 1(C) and (D), left). Correct targeting in all five clones was also confirmed by the appearance of a 3.8 kb *EcoRV* fragment by Southern blotting (a representative clone is shown in Fig. 1(D), right), and by additional blotting with *EGFP* sequences to identify clones carrying a single integration event (data not shown).

Expression of *EGFP* was assessed in the five targeted clones by fluorescence microscopy and by flow cytometry. Microscopic examination of wild type cells shows that none of the cells are significantly fluorescent, whereas nearly 100% of the cells expressing the *EGFP* coding sequence are brightly fluorescent (Fig. 1(E), top images). When analyzed by flow cytometry, a plot of relative fluorescence intensity per cell shows a wide range of natural fluorescence for wild type ES cells (Fig. 1(E), top left). Cells expressing *EGFP* fluoresce

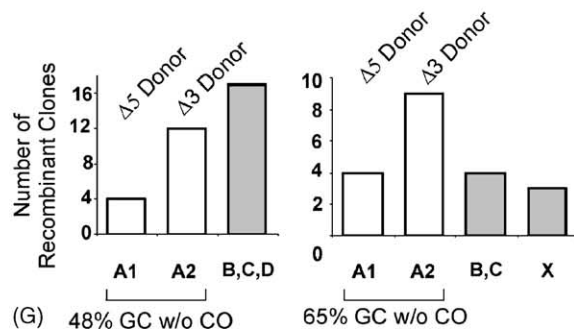
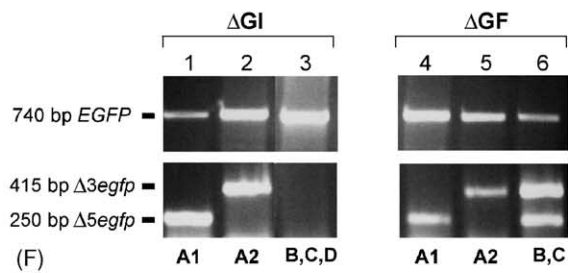
GENE CONVERSIONS WITHOUT CROSSOVERS



DELETIONS / INSERTIONS



Fluorescent Recombinant Clones



bright green and are shifted to the right (Fig. 1(E), top right). The fluorescence-positive R2 region was delineated to exclude all non-fluorescent cells while capturing most of the fluorescent cells. No fluorescent cells were observed in populations of either $\Delta 5egfp$ and $\Delta 3egfp$ clones, as expected (Fig. 1(E), middle). However, rare fluorescent cells were detected among ΔGI and ΔGF cells, both by flow cytometry and microscopy (Fig. 1(E), bottom), indicating that reconstitution of full length *EGFP* occurs only when mitotic homologous recombination is possible between the $\Delta 5egfp$ and $\Delta 3egfp$ cassettes.

To test the stability of *EGFP* expression at the ROSA26 locus, a positive control *EGFP* expressing clone was maintained in culture and periodically analyzed by flow cytometry. We did not observe any significant change in the percentage of fluorescent cells over the course of more than 3 weeks of continuous culturing (>30 doublings; data not shown), indicating that *EGFP* is stably expressed at this locus.

3.2. Distribution of spontaneous homologous recombination events in ΔGI and ΔGF

Restoration of full length *EGFP* in ΔGI or ΔGF cells can occur via various mechanisms of homologous recombination, and the outcomes can be classified broadly into two groups: conservative gene conversions (in which there is no associated crossing over), and non-conservative recombination events that are inevitably associated with deletions and insertions (Fig. 2). In conservative recombination at the ΔGI and ΔGF substrates, sequence information is transferred in a non-reciprocal fashion (gene conversion) and the overall arrangement of the DNA is conserved (Fig. 2(A)). The two major HDR pathways thought to cause gene conversions are SDSA and the prototypic break-repair model (if the Holliday junctions are resolved symmetrically). In contrast, alternative classes of recombination events result in a loss or a gain of one of the repeats in ΔGI and ΔGF , respectively. For example, *EGFP* can be restored by crossover of flanking sequences during unequal sister chromatid exchange (also called gene conversion with crossovers), resulting in a deletion in ΔGI and an expansion in ΔGF (Fig. 2(B)). In addition, replication fork repair (e.g., reconstitution of a broken replication

fork in a homologous-recombination dependent fashion) or long tract gene conversion similarly results in a deletion in ΔGI or an expansion in ΔGF (Fig. 2(C)). Finally, fluorescent recombinant cells that result from SSA can only arise in the ΔGI clone, since SSA in ΔGF produces a doubly mutant expression cassette (Fig. 2(D)).

In order to classify recombination events, PCR primers were designed to specifically detect full-length *EGFP*, $\Delta 3egfp$ and $\Delta 5egfp$. The presence of a full-length *EGFP* coding sequence was ascertained using primers that anneal to the undeleted 5' and 3' ends (Fig. 2(E)). During construction of the recombination substrates, unique sequences were inserted in place of each of the deleted regions within both $\Delta 3egfp$ and $\Delta 5egfp$. Using primers that anneal to these unique sequences, combined with primers that anneal to shared coding sequences, PCR products specific to $\Delta 3egfp$ and $\Delta 5egfp$ can be obtained (Fig. 1(E)). Each of the five targeted clones was then analyzed in parallel reactions, one to test for the presence of full length *EGFP*, and the other to assay for $\Delta 3egfp$ and $\Delta 5egfp$. As can be seen in Fig. 2(E) (lower panel), the positive control clone carries only full length *EGFP* (lane 1), each of the negative controls carries either $\Delta 3egfp$ or $\Delta 5egfp$ (lanes 2 and 3), and populations of unrecombined ΔGI and ΔGF cells show the presence of both $\Delta 5egfp$ and $\Delta 3egfp$, but not full length *EGFP* sequence, as expected (lanes 4 and 5).

To broadly classify clones as having undergone rearrangements that appear to be either gene conversions without crossovers or deletion/insertion events, we isolated spontaneous recombinants from multiple independent cultures by fluorescence activated cell sorting. Cells were expanded in culture, and analyzed for the presence of full length *EGFP*, $\Delta 3egfp$, and $\Delta 5egfp$ coding sequences. Examples of representative recombinant clones are shown in Fig. 2(F). For ΔGI , clones that have undergone a gene conversion without crossover have both full length *EGFP* and either $\Delta 3egfp$ or $\Delta 5egfp$ (Fig. 2(A) and (F), lanes 1 and 2). Alternative recombination pathways in ΔGI result in a deletion, detectable by the presence of full length *EGFP* coding sequences and the absence of both $\Delta 3egfp$ and $\Delta 5egfp$ (Fig. 2 (B)–(D) and (F), lane 3). For ΔGF , gene conversions without crossovers are classified using the same approach as for ΔGI (Fig. 2(A) and (F), lanes 4 and 5), however alternative pathways result in

Fig. 2. Delineation of the major HDR pathways in ΔGF and ΔGI . The expected arrangement of the DNA in recombinant cells expressing *EGFP* is shown (note that non-fluorescent daughter cells are not depicted). (A) Gene conversion without associated crossover of flanking sequences. (B–D) Alternative HDR pathways associated with either deletions or insertions: (B) unequal sister chromatid exchange (USCE), also termed gene conversion with crossover (GC-CO) reconstitutes *EGFP* in one of two daughter cells. Note that the product of a long tract gene conversion would be indistinguishable from this product. (C) Replication fork repair (RFR) is shown starting after replication fork breakdown in which a one-ended DSB appears. Note that this figure depicts events wherein the replication fork had been moving from left to right; *EGFP* can analogously be restored by repair of forks moving in the opposite direction (not shown). (D) SSA can reconstitute full length *EGFP* in ΔGI , but not in ΔGF . (E) Location of PCR primers and PCR products diagnostic of the pathways depicted in A–D. Arrows show expression cassette and gray regions depict coding sequence (not to scale). Black boxes depict deleted regions and each hatched box depicts a different unique sequence. Lower panel: Agarose gels showing PCR products from full length *EGFP* (top), $\Delta 3egfp$ and $\Delta 5egfp$ cassettes (bottom) amplified from genomic DNA isolated from the following correctly targeted clones: *EGFP* (lane 1), $\Delta 3egfp$ (lane 2), $\Delta 5egfp$ (lane 3), ΔGI (lane 4), ΔGF (lane 5). (F) PCR products from spontaneous recombinant clones isolated from ΔGI (left) and ΔGF (right). Representative recombinant clones showing gene conversion with $\Delta 5egfp$ as donor (lanes 1 and 4), gene conversion with $\Delta 3egfp$ as donor (lanes 2 and 5), USCE, RFR or SSA (lane 3), USCE or RFR (lane 6). (G) Number of independent recombinant clones from ΔGI (left) and ΔGF (right) showing mechanism A1 (gene conversion without crossover, $\Delta 5egfp$ as donor), A2 (gene conversion without crossover, $\Delta 3egfp$ as donor), B (USCE), C (RFR), D (SSA), and X (complex, not consistent with the major pathways depicted in A–D).

an expansion, revealed by the presence of full length *EGFP* and both $\Delta 3egfp$ and $\Delta 5egfp$ (Fig. 2 (B), (C) and (F), lane 6). Clones that did not fit these characteristics were classified as complex events. Eight independent clones were also analyzed by Southern blotting, and the arrangement of the DNA was exactly as expected based on the results of the PCR analysis (data not shown). This PCR approach thus provides an effective strategy for delineating the major classes of homologous recombination events that reconstitute *EGFP* coding sequences, making it possible to assess the proportion of recombination events due to gene conversion without crossovers versus other classes of events under spontaneous and damage-induced conditions.

To obtain a random sampling of spontaneous recombinant clones, >30 independent cultures of ΔGI and ΔGF were created by plating a low numbers of cells (~20,000) and allowing cells to expand over the course of approximately 1 week. To assure that only recombinants that arose during expansion were assessed, we eliminated cultures in which the frequency of recombinant cells indicated the existence of a pre-existing recombinant in the original inoculum (e.g., cultures with a frequency $\geq 1/20,000$). Spontaneous recombinant fluorescent cells were isolated from each culture by flow cytometry, and up to four independent clones were expanded in culture, and analyzed by PCR, as described above. If two recombinant clones from the same culture showed the same PCR result (which was often the case), it was counted as a single event, since recombinant cells in the same culture could have been derived from the same lineage. We tallied 33 and 20 independent recombination events in ΔGI and ΔGF , respectively. Note that we found that this diagnostic approach yielded highly consistent results, such that there was perfect concordance in over a dozen clones that were analyzed independently in a blinded fashion.

For ΔGI , we found that 48% of recombinant clones had undergone gene conversions without crossovers, in which $\Delta 5egfp$ donated sequences to $\Delta 3egfp$ in a non-reciprocal fashion, or vice versa (Fig. 2(G) left; A1 and A2). Similarly, we found that a significant proportion (65%) of the spontaneous ΔGF recombinants had undergone gene conversions without crossovers (Fig. 2(G) right; A1 and A2). Note that 15% of the spontaneous recombinant ΔGF clones had undergone complex recombination events (Fig. 2(G) right; X). Thus, taken together, we found that ~50–65% of the recombination events were gene conversions without crossovers in ΔGI and ΔGF , respectively, which is consistent with previous studies in which it has been reported that 50–100% spontaneous HDR events are gene conversions (the range in frequencies likely depends on intrinsic features of the recombination substrates and the cell type being studied) [28,29,34–36].

For both clones, gene conversions in which $\Delta 3egfp$ acted as the donor were detected somewhat more frequently than those in which $\Delta 5egfp$ acted as the donor (Fig. 2(G)). This result is likely due to the fact that a longer stretch of non-homologous sequence needs to participate in gene conversion events in which $\Delta 5egfp$ acts as the donor, which is con-

sistent with previous studies showing that gene conversions are increasingly suppressed by lengthening inserted non-homologous sequences [43]. In the context of these studies, the preference for $\Delta 3egfp$ over $\Delta 5egfp$ as the donor in gene conversions in both ΔGI and ΔGF indicates that sequences upstream and downstream of the recombination substrates (e.g., promoter sequences for nearby genes) do not impose a significant position effect (e.g., we did not see a preference for the upstream cassette acting as the donor, for example).

3.3. SSA is a commonly detected spontaneous recombination event in mouse ES cells

SSA events will only be detected in the ΔGI substrate (Fig. 2(D)). On the other hand, unequal sister chromatid exchanges and replication fork repair (Fig. 2, classes B and C) are detectable in both ΔGI and ΔGF . Therefore, the extent of SSA can be estimated by comparing the proportion of non-conservative recombination events that appear as either deletions (ΔGI) or expansions (ΔGF). We found that deletions and expansions accounted for 52% of the recombinants isolated from ΔGI , and 20% of the recombinants from ΔGF . Therefore, by subtraction, we estimate that ~30% of spontaneous recombination events are due to SSA (Fig. 2(G); subtraction of the BC classes of ΔGF from the BCD classes in ΔGI).

As an independent measure of the frequency of SSA, we compared the spontaneous rates of homologous recombination at the ΔGI and ΔGF substrates. We found that the rate of spontaneous HDR for two independent ΔGI clones was significantly higher than that of two independent ΔGF clones (Fig. 3(A); $p < 0.05$). This result is consistent with SSA events that are detectable for ΔGI , but not for ΔGF . To assess the global frequency of spontaneous homologous recombination, we assessed sister chromatid exchanges in metaphase spreads from one of each of the ΔGF and ΔGI clones (Fig. 3(B)).

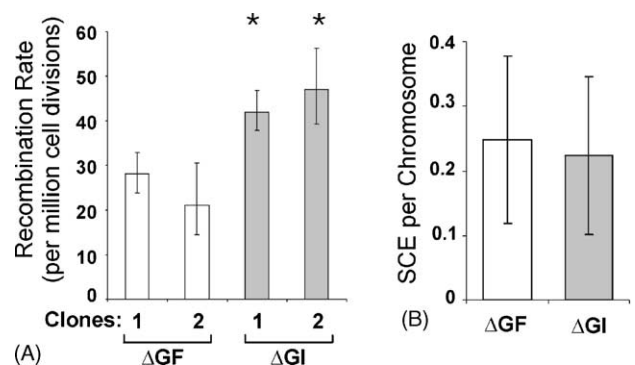


Fig. 3. Rate of spontaneous HDR at the recombination substrates and frequency of SCEs in metaphase spreads. (A) Rates of spontaneous recombination at the recombination substrates in two independent ΔGF clones (white) and two independent ΔGI clones (gray). Error bars indicate one standard deviation. (*) Rate of both ΔGI clones are statistically significantly greater than both of the ΔGF clones (Student's *T*-test, $p < 0.05$). (B) SCEs per chromosome in a ΔGI (white) and a ΔGF (gray) clone. Error bars indicate one standard deviation.

We found that there was no significant difference between these clones, indicating that a higher rate in the Δ GI clone is not due to intrinsic hyper-recombination. Taking the average spontaneous rates for each pair of independent clones, we found that there is a \sim 45% excess rate of spontaneous recombination in the Δ GI clones, which is attributable to SSA.

3.4. Mechanisms of ICL-induced homologous recombination

To explore the spectrum of recombination events induced by exposure to an agent that is thought to primarily induce one-ended DSBs, we exposed cells to MMC, an agent that creates ICLs. With increasing doses of MMC, we observed increasing toxicity (Fig. 4(A)). At 500 ng/ml, we observed a \sim 2.1- and a \sim 2.4-fold increase in the frequency of recombinant cells in Δ GF and Δ GI, respectively (Fig. 4(B)), thus demonstrating that exposure to MMC induces recombination in these clones. To determine the mechanisms of damage induced HDR, fluorescent recombinant cells were isolated from multiple independent MMC-exposed cultures, and the arrangement of the recombined DNA was analyzed by PCR, as described above.

In clones derived from MMC-exposed populations, the proportion of insertions in Δ GF increased significantly, from 35% to 60% (from 7/20 to 18/30) (Fig. 4(C) and (D)). These non-conservative events include complex events, which rose from 15% to 30% (from 3/20 to 9/30). Among Δ GF clones that had undergone gene conversions without crossovers, the frequency of gene conversions in which Δ 3*egfp* acted as the donor cassette was somewhat higher, which was also the case for spontaneous events. Among recombinants isolated from MMC-exposed Δ GI cultures, we observed a significant increase in the proportion of recombination events associated with deletions, rising from 52% to 90% (from 17/33 to 17/19) (Fig. 4(C) and (D)); note that there were no complex events among the Δ GI recombinant clones).

It noteworthy that it is possible that not all of the recombinant cells isolated from MMC-exposed cultures resulted from MMC induction. Based upon the frequency of recombinant cells present prior to plating (and taking into consideration the plating efficiency and the degree of MMC-induced toxicity), the expected proportion of MMC-exposed cultures carrying pre-existing recombinant cells is $<1/10$, which is not likely to significantly affect the results of these studies. However, it is possible that spontaneous recombinants arose during expansion of the MMC-exposed cultures, after the drug had been removed from the media. Consequently, if anything, we have underestimated the extent to which the spectrum of recombination events shifts following MMC exposure. Given that in both Δ GF and Δ GI we observed a statistically significant shift from gene conversions without crossovers to alternative pathways associated with insertions and deletions ($p < 0.05$; Fig. 4(D)), we conclude that MMC exposure increases the risk of deleterious recombination events, not just by causing

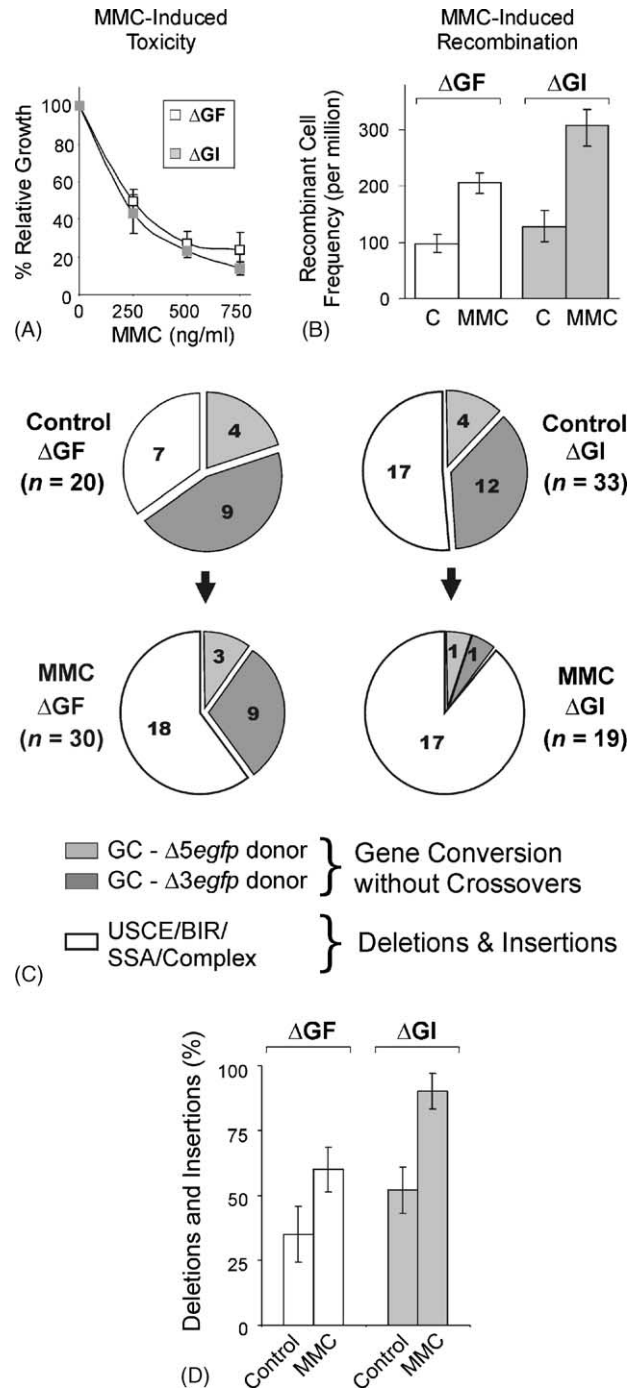


Fig. 4. Induction of HDR by exposure to MMC in Δ GF and Δ GI cells. (A) Relative growth of Δ GF (white) and Δ GI (gray) cells 48 h after exposure to the indicated doses of MMC. Error bars indicate one standard deviation of triplicate cultures. (B) Frequency of recombinant fluorescent cells in Δ GF (white) and Δ GI (gray) cells 48 h after exposure to MMC (500 ng/ml). Error bars indicate the standard deviation among six cultures. (C) Observed classes of recombination events among independent recombinant clones isolated from MMC-exposed Δ GF and Δ GI cells. The spectrum of spontaneous recombination events are included for comparison. (D) Percentage of recombinant cells in which recombination events are associated with deletions and insertions. The MMC-induced increase in the proportion of recombination events associated with deletions and insertions rises significantly in both the Δ GI and Δ GF clones ($p < 0.05$).

a general increase in the frequency of recombination, but also by increasing the proportion of recombination events that are associated with deletions and insertions.

4. Discussion

Although homologous recombination is known to cause sequence rearrangements that contribute to cancer, it is not yet known what causes spontaneous homologous recombination in mammals. The two major classes of lesions thought to initiate HDR events are one-ended DSBs, which arise as a consequence of replication fork breakdown, and two-ended DSBs, which can potentially arise in a replication-fork independent fashion. We are interested both in what causes spontaneous HDR, and in the possibility that exposure to exogenous DNA damaging agents might alter the proportion of HDR events associated with large scale sequence rearrangements. To explore these issues, we created recombination substrates that reveal the relative proportions of the major classes of recombination events. Using these substrates, we delineated the spectra of spontaneous events and events induced by exposure to an agent that induces ICLs, which inhibit replication fork progression. Two of the major findings of these studies are that (1) a significant proportion of spontaneous recombination events are consistent with induction by two-ended DSBs, and (2) exposure to an agent that induces ICLs significantly alters the spectrum of recombination events, causing a shift toward events that are associated with deletions and insertions.

In order to delineate the major classes of spontaneous and damage-induced recombination events, we created a pair of matched direct repeat recombination substrates. It is noteworthy that the design of a recombination substrate can profoundly influence the spectrum of observed events. For example, some substrates cannot detect short-tract gene conversions (e.g., [44]), while others have been designed to exclude SSA (e.g., [36]). Here, we describe the creation of substrates that detect all of the major classes of HDR events. Furthermore, by site specifically integrating a matched pair of substrates (wherein one detects SSA and the other does not), the contribution of SSA to spontaneous non-conservative recombination events can be revealed. The use of fluorescence as a marker for recombinant cells makes it possible to use flow cytometry to rapidly quantify recombinant cells in an automated fashion, and by inserting unique sequences into the deletion sites, the major classes of HDR can be delineated by PCR. Finally, by performing these studies in mouse ES cells, we can learn about recombination in untransformed mammalian cells.

SSA was first proposed as a model for repairing DSBs based on studies of extrachromosomal recombination products in mammalian cells [45], and it is now well established that SSA is a kinetically and genetically separable subpathway of HDR in *S. cerevisiae* [13,46]. Although it is widely held that SSA is also a subpathway of HDR in mammalian

cells, the frequency of spontaneous SSA in mammalian cells had not previously been reported, most likely because application of a single recombination reporter cannot distinguish SSA from other types of non-conservative HDR events. In previous studies by Bollag and Liskay, a matched pair of direct repeat substrates were created wherein one substrate detects SSA and the other does not [36]. Although the results of this previous study are consistent with the results presented here, showing an excess rate of ~50% due to SSA, their findings were inconclusive due to noise associated with random integration [36]. Additional substrates have been designed to detect SSA in mammalian cells, however, they have not been used to study spontaneous recombination events (i.e., these studies have focused on DSBs induced by a homing endonuclease) (e.g., [23]). Here, we have used a pair of targeted substrates to estimate the prevalence of spontaneous SSA events, and we found that ~30–50% of spontaneous recombination at these direct repeat substrates is due to SSA. It is expected that the frequency of SSA at a direct repeat will be highly variable, depending on both intrinsic factors (e.g., the length of the repeats) and extrinsic factors (e.g., the locus of integration). Nevertheless, these studies are valuable because they show that SSA can occur quite frequently in mammalian cells, which is of particular interest due to the fact that all models of SSA show that these events are initiated by two-ended DSBs. Therefore, the work presented here shows that spontaneous two-ended DSBs can contribute significantly to spontaneous homologous recombination events.

ICLs are thought to induce recombination by inhibiting replication fork progression. One possibility is that forks breakdown when single strand breaks are introduced at ICLs by ERCC1-XPF [47,48]. Another possibility is that DSBs arise when fork progression is inhibited [49], presumably due to fork regression leading to formation of Holliday junctions that are subsequently cleaved by resolvases, as has been shown to be the case in *Escherichia coli* [50]. The observations that most ICL-induced DSBs occur in a replication-dependent fashion [31–33] are consistent with induction of one-ended DSBs at replication forks. We reasoned that if most spontaneous homologous recombination events are stimulated by one-ended DSBs at replication forks, then exposure to an agent that creates ICLs would yield a spectrum similar to that of spontaneous HDR. However, the spectrum of spontaneous and ICL induced recombination events were significantly different from one another, which suggests that spontaneous recombination is often initiated by two-ended, rather than one-ended DSBs. This result is consistent with the conclusion from the SSA analysis that a significant proportion of spontaneous events stem from two-ended DSBs.

Intriguingly, we found that there was a modest but reproducible increase in the susceptibility of the Δ GI clone to MMC-induced recombination compared to the Δ GF clone, suggesting that exposure to MMC increases the frequency SSA. This was unexpected, since ICLs are not thought to

directly induce two-ended DSBs. One possibility is that some ICLs indeed lead to two-ended DSBs in a replication-independent fashion, which is supported by previous work in which pulse-field gel analysis shows a small but significant proportion of ICL-induced DSBs arising in arrested cells [31]. Another possibility is that if two forks converge at the same ICL, both can breakdown to create a two-ended DSB. Finally, it is also possible that some of the recombination events observed in the MMC-exposed cultures were not induced directly by ICLs, but instead indirectly resulted from either the associated redox potential of MMC which can lead to oxidative damage [51], or from a change in the state of the cells that renders them prone to HDR (perhaps due to the associated toxicity of the exposure) [52]. The latter is consistent with studies showing that thymidine induces HDR in the absence of detectable DSBs [53].

Several previous studies have investigated the effects of exogenous DNA damage on the spectrum of recombination events in mammalian cells. Two of particular relevance to this study investigated the effects of UV damage and phenytoin exposure, a chemical that induces reactive oxygen species [24,25]. In the UV study, it was found that most of the UV-induced recombination events were non-conservative [24]. Given that UV lesions are thought to induce HDR by inhibiting replication fork progression [54], these results are consistent with the work reported here. However, it should be noted that most of the spontaneous recombination events at this particular substrate were also non-conservative, so it did not appear that UV exposure significantly changed the proportion of non-conservative recombination events [24]. An additional study also supports the possibility that HDR induced by inhibition of replication forks is associated with exchanges [55], however the substrate used in this study is not amenable to comparisons between conservative short-tract gene conversions (without associated crossing), and other types of non-conservative HDR events. In a separate study of phenytoin-induced HDR, most of the induced events were conservative [25]. These results are consistent with the fact that oxidative damage can induce two-ended DSBs, and that enzymatically induced two-ended DSBs have been shown in several studies to primarily induce conservative gene conversion events [19–21,24]. Thus, together with the results presented here, it may be the case that exposure to agents that inhibit replication fork progress are associated with an increased risk of deleterious sequence rearrangements, though additional studies are clearly necessary to fully explore this possibility.

In this work, we have used direct repeat substrates to study the proportions of conservative and non-conservative recombination events. Although most HDR events in normal mammalian cells are not likely to occur at repeated sequences, these classifications nevertheless shed light on the prevalence of various mechanisms of recombination, some of which are more likely to be associated with deleterious rearrangements than others. For example, it is likely that SDSA is the underlying mechanism of a significant proportion of the conservative

recombination events in these studies [3]. SDSA is a relatively safe mechanism of HDR, since SDSA prevents crossovers, and crossovers between homologous chromosomes can cause LOH from the exchange point all the way to the telomere. In contrast, the non-conservative recombination events that appear as insertions and deletions at Δ GF and Δ GI are always associated with either crossovers or SSA, the former being associated with a risk of LOH, and the latter inevitably leading to loss of sequence information. Therefore, knowledge about the relative proportions of gene conversions without crossovers and recombination events associated with deletions and insertions yields valuable information about the extent to which the cell is performing HDR in a fashion that could lead to deleterious sequence rearrangements.

It is now broadly accepted that HDR processes are critical for maintenance of genomic integrity. Although HDR is essential for correct reinsertion of broken ends that arise during DNA replication, it is not known how often broken forks are the cause of spontaneous recombination events. Here, we show for the first time that SSA, a subpathway of HDR that is initiated by two-ended DSBs, is a common spontaneous recombination event in mammalian cells, which suggests that two-ended DSBs are the underlying cause of a significant proportion of spontaneous homologous recombination events. These results provide a valuable framework for future studies aimed at identifying the specific classes of DNA lesions that are likely to cause spontaneous two-ended DSBs. In addition, in this work we have shown that ICL exposure causes a significant shift in the spectrum of homologous recombination events, favoring non-conservative pathways that are associated with deletions and insertions. Loss of heterozygosity, deletions, insertions and translocations all can arise as a consequence of sequence exchanges during HDR. The results presented here therefore provide new information about how exposure to DNA damage can contribute to tumorigenic sequence rearrangements that potentially contribute to secondary tumors.

Acknowledgements

We are grateful to Dr. Andrew Engelward for help with statistical analysis for rate calculations, and to Dr. J. Nickoloff for helpful discussions and careful critique of this work. We thank Dr. E. Spek for suggestions in the design of the substrates, and to Jeffrey Loh and Jessica Lee for their valuable technical support. We thank the MIT Cancer Center for access to their flow cytometry core. We thank M. Okabe, P. Soriano, S. Srinivas, and F. Costantini for DNA vectors, with special thanks to the Soriano laboratory for exceptional technical resources made available for ROSA26 targeting. We thank Dr. R. Jaenisch for the J1 ES cells. This work was supported by R01CA79827 and R33 CA84740 with partial support from ES02109, P01-CA26735, and grants from Burroughs Wellcome Fund.

References

- [1] E.C. Friedberg, G.C. Walker, W. Siede, DNA Repair and Mutagenesis, ASM Press, Washington, DC, 1995.
- [2] A. Kuzminov, Recombinational Repair of DNA Damage, R.G. Landes Company, Austin, 1996.
- [3] F. Paques, J.E. Haber, Multiple pathways of recombination induced by double-strand breaks in *Saccharomyces cerevisiae*, Microbiol. Mol. Biol. Rev. 63 (1999) 349–404.
- [4] P. McGlynn, R.G. Lloyd, Recombinational repair and restart of damaged replication forks, Nat. Rev. Mol. Cell. Biol. 3 (2002) 859–870.
- [5] T. Helleday, Pathways for mitotic homologous recombination in mammalian cells, Mutation Res. 532 (2003) 103–115.
- [6] S.C. West, Molecular views of recombination proteins and their control, Nat. Rev. Mol. Cell. Biol. 4 (2003) 435–445.
- [7] J.O. Blaisdell, S.S. Wallace, Abortive base-excision repair of radiation-induced clustered DNA lesions in *Escherichia coli*, Proc. Natl. Acad. Sci. U.S.A. 98 (2001) 7426–7430.
- [8] B. Michel, G. Grompone, M.J. Flores, V. Bidnenko, Multiple pathways process stalled replication forks, Proc. Natl. Acad. Sci. U.S.A. 101 (2004) 12783–12788.
- [9] J.W. Szostak, T.L. Orr-Weaver, R.J. Rothstein, F.W. Stahl, The double-strand-break repair model for recombination, Cell 33 (1983) 25–35.
- [10] N. Nassif, J. Penney, S. Pal, W.R. Engels, G.B. Gloor, Efficient copying of nonhomologous sequences from ectopic sites via P-element-induced gap repair, Mol. Cell. Biol. 14 (1994) 1613–1625.
- [11] F. Paques, W.Y. Leung, J.E. Haber, Expansions and contractions in a tandem repeat induced by double-strand break repair, Mol. Cell. Biol. 18 (1998) 2045–2054.
- [12] R.A. Anderson, S.L. Eliason, Recombination of homologous DNA fragments transfected into mammalian cells occurs predominantly by terminal pairing, Mol. Cell. Biol. 6 (1986) 3246–3252.
- [13] J. Fishman-Lobell, N. Rudin, J.E. Haber, Two alternative pathways of double-strand break repair that are kinetically separable and independently modulated, Mol. Cell. Biol. 12 (1992) 1292–1303.
- [14] G. Luo, I.M. Santoro, L.D. McDaniel, I. Nishijima, M. Mills, H. Youssoufian, H. Vogel, R.A. Schultz, A. Bradley, Cancer predisposition caused by elevated mitotic recombination in Bloom mice, Nat. Genet. 26 (2000) 424–429.
- [15] A.J. Bishop, R.H. Schiestl, Homologous recombination as a mechanism for genome rearrangements: environmental and genetic effects, Hum. Mol. Genet. 9 (2000) 2427–2434.
- [16] D. Hellgren, Mutagen-induced recombination in mammalian cells in vitro, Mutation Res. 284 (1992) 37–51.
- [17] S. Lambert, Y. Saintigny, F. Delacote, F. Amiot, B. Chaput, M. Lecomte, S. Huck, P. Bertrand, B.S. Lopez, Analysis of intrachromosomal homologous recombination in mammalian cell, using tandem repeat sequences, Mutation Res. 433 (1999) 159–168.
- [18] J. Aubrecht, R. Rugo, R.H. Schiestl, Carcinogens induce intrachromosomal recombination in human cells, Carcinogenesis 16 (1995) 2841–2846.
- [19] D.G. Taghian, J.A. Nickoloff, Chromosomal double-strand breaks induce gene conversion at high frequency in mammalian cells, Mol. Cell. Biol. 17 (1997) 6386–6393.
- [20] R.G. Sargent, M.A. Brenneman, J.H. Wilson, Repair of site-specific double-strand breaks in a mammalian chromosome by homologous and illegitimate recombination, Mol. Cell. Biol. 17 (1997) 267–277.
- [21] Y. Lin, T. Lukacovich, A.S. Waldman, Multiple pathways for repair of DNA double-strand breaks in mammalian chromosomes, Mol. Cell. Biol. 19 (1999) 8353–8360.
- [22] B. Elliott, C. Richardson, J. Winderbaum, J.A. Nickoloff, M. Jasin, Gene conversion tracts from double-strand break repair in mammalian cells, Mol. Cell. Biol. 18 (1998) 93–101.
- [23] M.L. Dronkert, H.B. Beverloo, R.D. Johnson, J.H. Hoeijmakers, M. Jasin, R. Kanaar, Mouse RAD54 affects DNA double-strand break repair and sister chromatid exchange, Mol. Cell. Biol. 20 (2000) 3147–3156.
- [24] C.A. Bill, J.A. Nickoloff, Spontaneous and ultraviolet light-induced direct repeat recombination in mammalian cells frequently results in repeat deletion, Mutation Res. 487 (2001) 41–50.
- [25] L.M. Winn, P.M. Kim, J.A. Nickoloff, Oxidative stress-induced homologous recombination as a novel mechanism for phenytoin-initiated toxicity, J. Pharmacol. Exp. Ther. 2 (2003) 523–527.
- [26] V.W. Liu-Lee, J.A. Heddle, C.F. Arlett, B. Broughton, Genetic effects of specific DNA lesions in mammalian cells, Mutation Res. 127 (1984) 139–147.
- [27] Y.Y. Wang, V.M. Maher, R.M. Liskay, J.J. McCormick, Carcinogens can induce homologous recombination between duplicated chromosomal sequences in mouse L cells, Mol. Cell. Biol. 8 (1988) 196–202.
- [28] F. Larminat, M. Germanier, E. Papouli, M. Defais, Impairment of homologous recombination control in a Fanconi anemia-like Chinese hamster cell mutant, Biol. Cell 96 (2004) 545–552.
- [29] F. Larminat, M. Germanier, E. Papouli, M. Defais, Deficiency in BRCA2 leads to increase in non-conservative homologous recombination, Oncogene 21 (2002) 5188–5192.
- [30] P.J. McHugh, V.J. Spanswick, J.A. Hartley, Repair of DNA interstrand crosslinks: molecular mechanisms and clinical relevance, Lancet Oncol. 2 (2001) 483–490.
- [31] I.U. De Silva, P.J. McHugh, P.H. Clingen, J.A. Hartley, Defining the roles of nucleotide excision repair and recombination in the repair of DNA interstrand cross-links in mammalian cells, Mol. Cell. Biol. 20 (2000) 7980–7990.
- [32] A. Rothfuss, M. Grompe, Repair kinetics of genomic interstrand DNA cross-links: evidence for DNA double-strand break-dependent activation of the Fanconi anemia/BRCA pathway, Mol. Cell. Biol. 24 (2004) 123–134.
- [33] L.J. Niedernhofer, H. Odijk, M. Budzowska, E. van Drunen, A. Maas, A.F. Theil, J. de Wit, N.G. Jaspers, H.B. Beverloo, J.H. Hoeijmakers, R. Kanaar, The structure-specific endonuclease Ercc1-Xpf is required to resolve DNA interstrand cross-link-induced double-strand breaks, Mol. Cell. Biol. 24 (2004) 5776–5787.
- [34] R.M. Liskay, J.L. Stachelek, A. Letsou, Homologous recombination between repeated chromosomal sequences in mouse cells, Cold Spring Harb. Symp. Quant. Biol. 49 (1984) 183–189.
- [35] R.J. Bollag, R.M. Liskay, Conservative intrachromosomal recombination between inverted repeats in mouse cells: association between reciprocal exchange and gene conversion, Genetics 119 (1988) 161–169.
- [36] R.J. Bollag, R.M. Liskay, Direct-repeat analysis of chromatid interactions during intrachromosomal recombination in mouse cells, Mol. Cell. Biol. 11 (1991) 4839–4845.
- [37] M. Okabe, M. Ikawa, K. Kominami, T. Nakanishi, Y. Nishimune, ‘Green mice’ as a source of ubiquitous green cells, FEBS Lett. 407 (1997) 313–319.
- [38] P. Soriano, Generalized *lacZ* expression with the ROSA26 Cre reporter strain, Nat. Genet. 21 (1999) 70–71.
- [39] S. Srinivas, T. Watanabe, C.S. Lin, C.M. William, Y. Tanabe, T.M. Jessell, F. Costantini, Cre reporter strains produced by targeted insertion of *EYFP* and *ECFP* into the *ROSA26* locus, BMC Dev. Biol. 1 (2001) 4.
- [40] W.A. Rosche, P.L. Foster, Determining mutation rates in bacterial populations, Methods 20 (2000) 4–17.
- [41] R.W. Sobol, M. Kartalou, K.H. Almeida, D.F. Joyce, B.P. Engelward, J.K. Horton, R. Prasad, L.D. Samson, S.H. Wilson, Base excision repair intermediates induce p53-independent cytotoxic and genotoxic responses, J. Biol. Chem. 278 (2003) 39951–39959.
- [42] J. Dopf, T.M. Horiagon, Deletion mapping of the *Aequorea victoria* green fluorescent protein, Gene 173 (1996) 39–44.
- [43] A.R. Godwin, R.M. Liskay, The effects of insertions on mammalian intrachromosomal recombination, Genetics 136 (1994) 607–617.

- [44] Y. Gondo, J.M. Gardner, Y. Nakatsu, D. Durham-Pierre, S.A. Deveau, C. Kuper, M.H. Brilliant, High-frequency genetic reversion mediated by a DNA duplication: the mouse pink-eyed unstable mutation, *Proc. Natl. Acad. Sci. U.S.A.* 90 (1993) 297–301.
- [45] F.L. Lin, K. Sperle, N. Sternberg, Model for homologous recombination during transfer of DNA into mouse L cells: role for DNA ends in the recombination process, *Mol. Cell. Biol.* 4 (1984) 1020–1034.
- [46] J. Fishman-Lobell, J.E. Haber, Removal of nonhomologous DNA ends in double-strand break recombination: the role of the yeast ultraviolet repair gene RAD1, *Science* 258 (1992) 480–484.
- [47] D. Mu, T. Bessho, L.V. Nechev, D.J. Chen, T.M. Harris, J.E. Hearst, A. Sancar, DNA interstrand cross-links induce futile repair synthesis in mammalian cell extracts, *Mol. Cell. Biol.* 20 (2000) 2446–2454.
- [48] I. Kuraoka, W.R. Kobertz, R.R. Ariza, M. Biggerstaff, J.M. Essigmann, R.D. Wood, Repair of an interstrand DNA cross-link initiated by ERCC1-XPF repair/recombination nuclease, *J. Biol. Chem.* 275 (2000) 26632–26636.
- [49] Y. Saintigny, F. Delacote, G. Vares, F. Petitot, S. Lambert, D. Averbeck, B.S. Lopez, Characterization of homologous recombination induced by replication inhibition in mammalian cells, *EMBO J.* 20 (2001) 3861–3870.
- [50] B. Michel, M.J. Flores, E. Viguera, G. Grompone, M. Seigneur, V. Bidnenko, Rescue of arrested replication forks by homologous recombination, *Proc. Natl. Acad. Sci. U.S.A.* 98 (2001) 8181–8188.
- [51] A.E. Maccubbin, N. Ersing, E.E. Budzinski, H.C. Box, H.L. Gurttoo, Formation of 8-hydroxyguanine in DNA during mitomycin C activation, *Cancer Biochem. Biophys.* 14 (1994) 1831–1891.
- [52] C. Hoege, B. Pfander, G.L. Moldovan, G. Pyrowolakis, S. Jentsch, RAD6-dependent DNA repair is linked to modification of PCNA by ubiquitin and SUMO, *Nature* 419 (2002) 135–141.
- [53] C. Lundin, K. Erixon, C. Arnaudeau, N. Schultz, D. Jenssen, M. Meuth, T. Helleday, Different roles for nonhomologous end joining and homologous recombination following replication arrest in mammalian cells, *Mol. Cell. Biol.* 22 (2002) 5869–5878.
- [54] T. Tsujimura, V.M. Maher, A.R. Godwin, R.M. Liskay, J.J. McCormick, Frequency of intrachromosomal homologous recombination induced by UV radiation in normally repairing and excision repair-deficient human cells, *Proc. Natl. Acad. Sci. U.S.A.* 87 (1990) 1566–1570.
- [55] C. Arnaudeau, C. Lundin, T. Helleday, DNA double-strand breaks associated with replication forks are predominantly repaired by homologous recombination involving an exchange mechanism in mammalian cells, *J. Mol. Biol.* 307 (2001) 1235–1245.